Available online at www.sciencedirect.com
SCIENCE DIRECT®
International Journal of Thermal Sciences 45 (2006) 969–976
International Journal of Thermal Sciences
www.elsevier.com/locate/ijts

Transient simulation of reacting radiating flows

A. Bilge Uygur, Tanil Tarhan, Nevin Selçuk *

Department of Chemical Engineering, Middle East Technical University, 06531 Ankara, Turkey

Received 25 October 2005; accepted 12 January 2006
Available online 17 February 2006

Abstract

Laminar methane–air diffusion flame was simulated by coupling a method of lines based parallel direct numerical simulation code with a radiation code based on method of lines solution of discrete ordinates method. The predictions of the code are validated against experimental data as well as numerical results of the same code without radiation model. Comparisons show that incorporation of radiation code to the computational fluid dynamics code results in a significant improvement in the predicted temperatures. Transient results exhibit the physically expected trends. The coupled code is a promising tool for the simulation of transient reacting radiating flows.

Keywords: Unsteady diffusion flames; Reacting radiating flows; Method of Lines (MOL); Parallel algorithms

1. Introduction

Combustion processes are essential for power generation, since an overwhelming majority of energy-producing devices rely on the combustion of fossil or renewable fuels. In many of these applications reactants are not initially mixed (non-premixed) and the flow field in which chemical reactions take place is turbulent. Due to a growing awareness concerning combustion related pollutant emissions, there is an increasing need towards optimization of these systems. Because of the high cost of experimental testing and prototyping, numerical simulations become more and more important to investigate non-premixed combustion by increasing our understanding of flame structures and dynamics [1].

Numerical simulation of unsteady diffusion flames is characterized by the very different time and space scales controlling physical and chemical processes. The physical and chemical processes can cover time scales ranging over nine orders of magnitude and space scales ranging over five orders of magnitude [2]. Moreover, incorporation of detailed reaction mechanisms and radiation models with varying complexity in the simulation of these flames results in large number of equations to be solved in conjunction with the other conservation equations and hence in excessive computation times. Therefore today's limited computer resources together with the difficulties listed above generally enforces the researchers to make a compromise between the level of detail of reaction mechanism and incorporation of models for radiation transport and soot formation.

The requirement for accurate predictions on one hand and the complex nature of the phenomenon on the other, modelling of diffusion flames has been a scientific challenge, a task which has been the subject of various studies [2–5]. In a such study, the effect of radiation and soot models on transient simulation of ethylene–air diffusion flames whilst using a single step reaction mechanism was investigated by Kaplan et al. [2]. In another study, Bedat et al. [3] performed direct simulation of turbulent methane–air diffusion flames using a four-step reaction mechanism including NO_x formation. Favorable comparisons between the predictions of a detailed GRI 2.11 mechanism and that obtained by the four-step reduced mechanism were reported. Coelho et al. [4] on the other hand, performed steady simulations of a turbulent jet diffusion flame, on which experimental data is available, using conserved scalar approach. Both gray and non-gray radiation models were employed in the computations. Despite the fact that results obtained for non-gray case were found to be closer to experimental data, radiative heat loss was significantly overestimated in both cases. What all above listed studies [2–5] have in common is that they point

* Corresponding author.
E-mail address: selcuk@metu.edu.tr (N. Selçuk).

1290-0729/$ – see front matter
doi:10.1016/j.ijthermalsci.2006.01.008

Nomenclature

$\widehat{C}_p$	specific heat capacity
D	diffusion coefficient
g	gravitational acceleration
$\widehat{H}$	enthalpy
I	radiative intensity
j	mass flux
u	axial component of the velocity
v	radial component of the velocity
p	pressure
q	heat flux
r	radial distance
t	time
T	temperature
Y	species mass fraction
z	axial distance

Greek letters

λ	thermal conductivity
μ	viscosity; direction cosine with respect to r axis
ρ	density
ξ	direction cosine with respect to z axis
$\dot{\omega}$	rate of reaction

Subscripts

A	air
F	fuel
in	inlet
k	species
km	mixture-averaged
p	print
ref	reference
w	wall

Superscripts

m	index for levels of ordinates at constant polar angle
l	index for ordinates at level m
$+$	positive direction
$-$	negative direction

out to the fact that incorporation of radiation transport is crucial for the simulation of diffusion flames.

Prediction of the behaviour of diffusion flames, on the other hand, necessitates an accurate and efficient determination of the flow field. Research carried out over the past two decades reveals that DNS is the most accurate approach for the prediction of laminar and turbulent flows [1,3]. However, due to the fact that a lot of grid points as well as time steps are needed for the direct simulation of turbulent flows, both accurate and efficient numerical techniques, and high performance computers are required for the simulation in acceptable computation times. The former can be achieved by increasing the order of the spatial discretization method, resulting in high accuracy with less grid points, and using not only a highly accurate but also a stable numerical algorithm for the time integration. The Method of Lines (MOL) [6] is an alternative approach that meets this requirement for time dependent problems. The latter requirement is met by either supercomputers or parallel computers which require efficient parallel algorithms.

A novel CFD code based on MOL for the DNS of 2D incompressible separated internal non-isothermal flows in regular and complex geometries was first developed by Oymak and Selçuk [7,8]. The code uses the MOL approach in conjunction with (i) higher-order spatial discretization scheme which chooses biased-upwind and biased-downwind discretization in a zone of dependence manner, (ii) a parabolic algorithm which removes the necessity of iterative solution for pressure (iii) an elliptic grid generator using body-fitted curvilinear coordinate system for application to complex geometries. The validity and the predictive ability of the code was tested by applying it to the simulation of laminar/turbulent, isothermal/non-isothermal incompressible flows and comparing its predictions with either measured data or numerical simulations available in the literature [9,10]. In a latter study by the same group [11], finite rate chemistry was incorporated to the above-mentioned code in order to simulate 2D transient laminar non-radiating reacting flows as an initial step towards the direct simulation of turbulent reacting radiating flows. While inheriting the key features of its predecessor, the latter code possesses some new features such as (i) a TVD based spatial discretization scheme which chooses biased-upwind and biased-downwind discretization in a zone of dependence manner, (ii) finite rate chemistry model (iii) domain decomposition based parallelization strategy. The predictive accuracy of the code was tested by applying it to the simulation of a confined laminar methane/air diffusion flame and comparing its predictions with numerical and experimental data available in the literature [12]. The predicted velocity, temperature and major species concentrations were found to be in reasonably good agreement with measurements.

Although the approaches without radiation transport aid in understanding some aspects of diffusion flames, radiative heat transfer effects should be taken into consideration for a better representation of these systems. This paper describes incorporation of an existing radiation code based on MOL solution of Discrete Ordinates Method (DOM) [13–16] to a MOL based parallel DNS code [11] for the simulation of methane–air confined diffusion flames using a recently proposed methodology described in [17]. To the authors' knowledge, a parallel implemented MOL based DNS code in conjunction with a model for radiation transport for the simulation of transient laminar reacting flows is not available to date.

2. Numerical solution technique

The physical situation under consideration is unsteady, confined, axisymmetric, laminar methane–air diffusion flame. The assumptions underlying the present analysis are as follows: (i) the flow is incompressible with temperature and pressure

dependent thermophysical properties, (ii) the methane–air reaction can be represented using a one step reaction mechanism by Khalil et al. [18] in order to make the coupled code less CPU intensive (iii) the reaction mixture is gray, absorbing and emitting medium and (iv) the boundaries are gray and diffuse.

The unsteady modelling of this system requires solution of conservation equations of mass, momentum, energy and species in conjunction with the radiative transfer equation. The methodology presented in this study is based on the coupling between a MOL based parallel DNS code and a radiation code based on the MOL solution of DOM.

The MOL which is a semi-discrete approach for the solution of time-dependent partial differential equations (PDE) consists of two stages. First, the dependent variables are kept continuous in time and the PDEs are discretized only in space on a dimension by dimension basis using any readily available 1-D spatial discretization package such as finite difference, finite volume or finite element based schemes. This leads to a system of ordinary differential equations (ODE) to be integrated in time using any readily available explicit or implicit ODE solvers, constituting the second stage. By this way, MOL not only offers accurate and stable solutions but also flexibility to incorporate any desired package with ease.

In what follows, the respective codes and the coupling procedure will be described.

2.1. Description of the CFD code

The conservation equations for transient 2-D incompressible reacting flows in cylindrical coordinates are as follows:

continuity:

$$\frac{\partial u}{\partial z}+\frac{v}{r}+\frac{\partial v}{\partial r}=0 \tag{1}$$

z-momentum:

$$\begin{aligned}&\frac{\partial u}{\partial t}+u\frac{\partial u}{\partial z}+v\frac{\partial u}{\partial r}\\&\quad=-\frac{1}{\rho}\frac{\partial p}{\partial z}+\frac{\mu}{\rho}\left(\frac{\partial^2 u}{\partial r^2}+\frac{1}{r}\frac{\partial u}{\partial r}+\frac{\partial^2 u}{\partial z^2}\right)\\&\qquad+\frac{1}{\rho}\left(\frac{\partial u}{\partial r}+\frac{\partial v}{\partial z}\right)\frac{\partial \mu}{\partial r}+\frac{2}{\rho}\left(\frac{\partial u}{\partial z}\right)\frac{\partial \mu}{\partial z}+g_z\end{aligned} \tag{2}$$

r-momentum:

$$\begin{aligned}&\frac{\partial v}{\partial t}+u\frac{\partial v}{\partial z}+v\frac{\partial v}{\partial r}\\&\quad=-\frac{1}{\rho}\frac{\partial p}{\partial r}+\frac{\mu}{\rho}\left(\frac{\partial^2 v}{\partial r^2}+\frac{1}{r}\frac{\partial v}{\partial r}-\frac{v}{r^2}+\frac{\partial^2 v}{\partial z^2}\right)\\&\qquad+\frac{2}{\rho}\left(\frac{\partial v}{\partial r}\right)\frac{\partial \mu}{\partial r}+\frac{1}{\rho}\left(\frac{\partial u}{\partial r}+\frac{\partial v}{\partial z}\right)\frac{\partial \mu}{\partial z}+g_r\end{aligned} \tag{3}$$

energy:

$$\begin{aligned}&\frac{\partial T}{\partial t}+u\frac{\partial T}{\partial z}+v\frac{\partial T}{\partial r}\\&\quad=\frac{\lambda}{\rho\widehat{C}_p}\left(\frac{\partial^2 T}{\partial r^2}+\frac{1}{r}\frac{\partial T}{\partial r}+\frac{\partial^2 T}{\partial z^2}\right)\\&\qquad+\frac{1}{\rho\widehat{C}_p}\left(\frac{\partial T}{\partial r}\right)\frac{\partial \lambda}{\partial r}+\frac{1}{\rho\widehat{C}_p}\left(\frac{\partial T}{\partial z}\right)\frac{\partial \lambda}{\partial z}\\&\qquad-\frac{1}{\rho\widehat{C}_p}\sum_{k=1}^{N}\widehat{C}_{p,k}\left(j_{k,r}\frac{\partial T}{\partial r}+j_{k,z}\frac{\partial T}{\partial z}\right)\\&\qquad-\frac{1}{\rho\widehat{C}_p}\sum_{k=1}^{N}\widehat{H}_k\dot{\omega}_k-\frac{\nabla\cdot q_R}{\rho\hat{C}_p}\end{aligned} \tag{4}$$

species:

$$\begin{aligned}&\frac{\partial Y_k}{\partial t}+u\frac{\partial Y_k}{\partial z}+v\frac{\partial Y_k}{\partial r}\\&\quad=-\frac{1}{\rho}\left(\frac{\partial j_{k,r}}{\partial r}+\frac{j_{k,r}}{r}+\frac{\partial j_{k,z}}{\partial z}\right)+\frac{\dot{\omega}_k}{\rho}\end{aligned} \tag{5}$$

While solving above-listed equations, transport properties, namely, viscosity, thermal conductivity and diffusion coefficients are calculated using the TRANSPORT package by Kee et al. [19]. Diffusive mass fluxes are computed using a Fickian type expression. Thermodynamic properties, namely, density and specific heat are evaluated using CHEMKIN-III [20] and its database. Coupling between the CFD and radiation codes is established through the divergence of radiative heat flux term in Eq. (4). The initial and boundary conditions used in the solution of Eqs. (1)–(5) are shown in Table 1.

Here, BC1, BC2 and BC3 represent axial symmetry, no slip at the wall and specified velocity, temperature and species profiles at the inlet, respectively. BC4, also known as the soft boundary condition, describes the developing flow.

In this study, for the numerical solution of the conservation equations, a previously developed MOL based DNS code [7] which has been extended to reacting flows by Tarhan [11] is used. Details of the algorithm can be found elsewhere [11,21].

2.2. Description of the radiation code

Solution of the RTE is based on MOL solution of DOM which was previously developed and applied to the simulation of steady-state radiative transfer in 2-D axisymmetric, absorbing, emitting, gray media [16]. The solution of discrete

Table 1
Initial and boundary conditions for the CFD code

IC:	@ $t=0$,	$\forall z \Lambda \forall r$:	$u=0$,	$v=0$,	$T=T_{\text{ref}}$,	$Y_k=Y_{k,0}$,	$\nabla\cdot q_R=0$
BC1:	@ $r=0$,	$\forall z \Lambda \forall t$:	$\frac{\partial u}{\partial r}=0$,	$v=0$,	$\frac{\partial T}{\partial r}=0$,	$\frac{\partial Y_k}{\partial r}=0$	
BC2:	@ $r=R$,	$\forall z \Lambda \forall t$:	$u=0$,	$v=0$,	$T=T_{\text{wall}}$,	$\frac{\partial Y_k}{\partial r}=0$	
BC3:	@ $z=0$,	$\forall r \Lambda \forall t$:	$u=u_{\text{in}}$,	$v=0$,	$T=T_{\text{in}}$,	$Y_k=Y_{k,\text{in}}$	
BC4:	@ $z=L$,	$\forall r \Lambda \forall t$:	$\frac{\partial^2 u}{\partial z^2}=0$,	$\frac{\partial^2 v}{\partial z^2}=0$,	$\frac{\partial^2 T}{\partial z^2}=0$,	$\frac{\partial j_k}{\partial z}=0$	

ordinates equations with MOL is carried out by adoption of the false-transients approach which involves incorporation of a pseudo-time derivative of intensity. Application of the false-transients approach to the discrete ordinates representation of RTE yields,

$$k_{t^*}\frac{\partial I^{m,l}}{\partial t^*} = -\frac{\mu_{m,l}}{r}\frac{\partial (r I^{m,l})}{\partial r} + \frac{1}{r}\frac{(\gamma_{m,l+1/2} I^{m,l+1/2} - \gamma_{m,l-1/2} I^{m,l-1/2})}{w_{m,l}} - \xi_{m,l}\frac{\partial I^{m,l}}{\partial z} - \kappa I^{m,l} + \kappa\frac{\sigma T^4}{\pi} \quad (6)$$

where the first term is the pseudo-time derivative, t^* is the artificial time variable and k_{t^*} is a time constant with dimension $(\mathrm{m/s})^{-1}$ which is taken as unity. The first three terms on the right-hand side stand for the gradient of intensity in curvilinear coordinates. The second term is an approximation for the angular derivative term which accounts for the variation of the direction of the coordinate system with respect to ordinate direction as radiation propagates in cylindrical coordinates. The angular redistribution terms, $\gamma_{m,l\pm1/2}$, depend on the selected quadrature set and are calculated for each angular range from a recurrence relation derived from the principle of conservation of energy in a uniform intensity condition. $I^{m,l+1/2}[= (I^{m,l} + I^{m,l+1})/2]$ and $I^{m,l-1/2}[= (I^{m,l-1} + I^{m,l})/2]$ define the intensities at edges of angular range of $w_{m,l}$. Further details of angular redistribution terms and estimation of the angular derivative can be found from [16]. The last two terms on the RHS are the absorption and emission terms. The inlet and exit boundaries were assumed to be black walls at gas and wall temperatures provided by the fluid flow code. The wall at $r = R$ was represented by a black boundary with specified temperature.

Following the MOL approach, the system of PDEs, Eq. (6), is then transformed into an ODE initial-value problem by representation of the spatial derivatives with algebraic finite-difference approximations. Starting from an initial condition for radiation intensities in all directions, the resulting ODE system is integrated until steady-state by using a powerful ODE solver. Any initial condition can be chosen to start the integration, as its effect on the steady-state solution decays to insignificance. To stop the integration at steady-state, a convergence criterion is checked for all intensities.

Once the discrete ordinate intensities at all grid points are available, the divergence of radiative heat flux can be obtained from Eq. (7).

$$\nabla \cdot q_R = \kappa\left(4\sigma T^4 - \sum_m \sum_l w_{m,l} I^{m,l}\right) \quad (7)$$

The performance of this radiation code was assessed on various test cases by comparing its steady-state predictions with exact solutions or experimental data available in the literature [16]. Comparisons show that the model provides accurate solutions for radiative heat fluxes and source terms and can be used with confidence in conjunction with CFD codes based on the same approach.

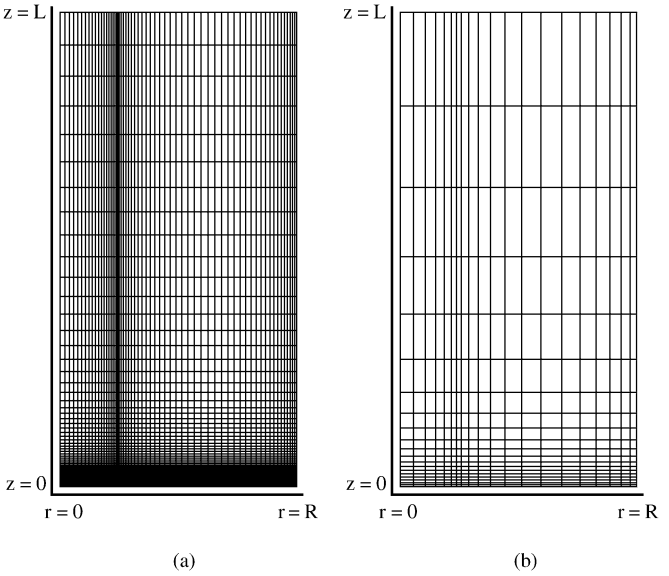

Fig. 1. Representative grid structure: (a) CFD; (b) Radiation.

In the present study, this radiation code was implemented by using two-point upwind differencing scheme and a non-uniform grid structure determined by the flow code. The S4 order of approximation was found to be optimum by successive refinement studies. RKF45 (Runge–Kutta–Fehlberg integration) subroutine which is an adaptive, 4th order accurate ODE solver was utilized. The temperature and concentration dependent absorption coefficients for the gray gas were calculated using Leckner's correlations [22].

2.3. Description of the coupling procedure for CFD and radiation codes

Coupling strategy between the CFD and radiation codes is mainly based on regular transfer of temperature field solved by the CFD code to the radiation code which in turn provides source term field for the energy equation as solution propagates in time. The algorithm starts with the specification of the initial conditions and grid structure for the numerical solution. A variable mesh size in both r and z directions was used which are clustered to the wall in r and to the inlet in z directions, respectively (Fig. 1). Owing to the nature of radiation transport, radiative heat transfer computations can be performed on much coarser grid resolutions when compared to that required for fluid flow. Hence instead of using identical grid resolutions for both fluid flow and radiation transport, two different grid resolutions were utilized; a fine mesh for fluid flow and a coarse one enabling economic computation of radiative source term.

With the initial conditions, CFD code advances one time step t_p, and makes flow and temperature fields available. Temperatures at the overlapping grid points of the coarse and fine meshes are transferred to the radiation code which in turn provides radiative energy source term at the same grid points for the CFD code. Source terms on the coarse mesh are redistributed to fine mesh of the CFD code via 2-D interpolation. With these source terms CFD code continues marching in time. Upon

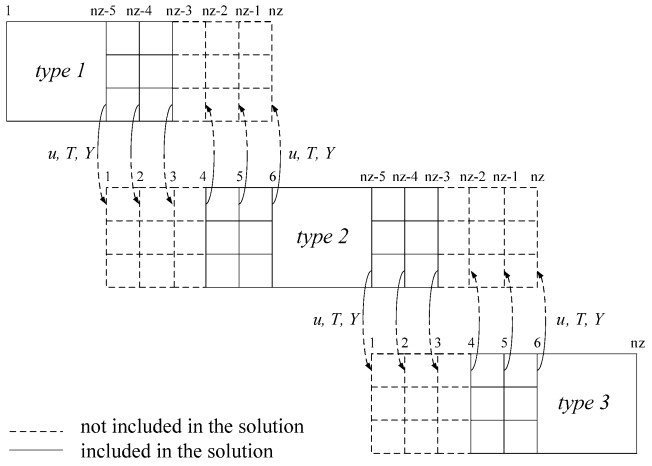

Fig. 2. Three point exchange with six points overlap paradigm for the CFD code.

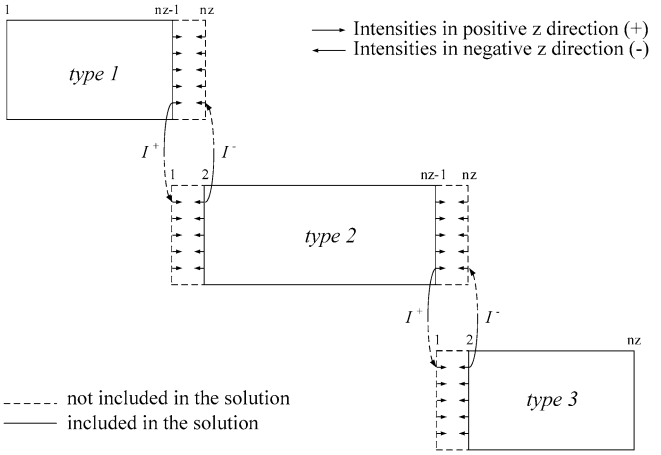

Fig. 3. One point intensity exchange with two points overlap paradigm for the radiation code.

the next call, the radiation code commences with the final intensities from the previous call to obtain faster convergence. It is worth noting here that t_p is not necessarily equal to the internal time step chosen by the ODE solver. The ODE solver chooses much smaller internal time steps than t_p. Another role attributed to t_p other than being the time interval at which the code produces output is that, the same source term field for the solution of energy equation is used throughout the interval t_p, an approach which significantly reduces the CPU time of the code without any compromise from accuracy. This cyclic procedure is repeated until steady-state solution is obtained.

3. Parallel implementation of the coupled code

Parallelization of the existing sequential codes and executing them on personal computer (PC) clusters is an economic approach to perform diffusion flame simulations in reasonable computation times.

In the present study, parallel implementation was carried out using domain decomposition technique by means of overlapping boundaries at the intergrid regions together with the PVM message passing software due to their proven feasibilities in CFD codes [10,11,23]. The algorithm is based on the master-slave paradigm, where the master process generates the grid structure, sets the initial and physical boundary conditions, decomposes the domain into sub-domains having the same number of grid points, sets the type of each sub-domain (*type*) and sends the related information to the slave processes. The type of sub-domain is determined according to the position of that sub-domain relative to the others (Fig. 2). The leftmost sub-domain is assigned as *type-1*, which includes an inlet boundary condition and an imaginary boundary condition; the rightmost sub-domain is assigned as *type-3*, which includes an imaginary condition and an outlet boundary condition; and the intermediate sub-domains are assigned as *type-2*, which include two imaginary boundary conditions. The slave processes perform the calculations for the sub-domains assigned to them according to the types set by the master process, advance in time and exchange necessary information between each other at user defined time steps (t_p) and send transient results to the master process for the development of the transient solution until steady state is reached.

At this point it is believed that the concept of information exchange between the subdomains should be explained in more detail since it constitutes the core of domain decomposition technique. The variables to be exchanged are axial velocity (u), temperature (T) and species mole fractions (Y) for the CFD code and radiative intensity (I) for the radiation code. 5-point discretization scheme based on biased-upwind or biased-downwind stencils used in the CFD code and 2-point upwind discretization scheme used in the radiation code, necessitates, at least three points for the CFD code (Fig. 2) and one point for the radiation code (Fig. 3) to be exchanged between the neighboring sub-domains at user defined time steps. Examination of Fig. 3 reveals that in order that the intensities in the domain of *type-1* (left domain) feel the effect of the intensity field in the domain of *type-2* (right domain), the intensities at the boundaries with negative z direction should be transferred from right to left and vice versa rather than transferring the intensities at all directions.

4. Results

The predictive performance of the parallel code was assessed on the laminar methane–air diffusion flame problem which has been previously studied in [11,12] (Fig. 4). Predictions of the present code are benchmarked against both the numerical results of [11] obtained in the absence of radiative heat transfer and experimental data reported in [12]. ROWMAP [24] was used as an ODE solver with the minimum internal time step being in the order of 1×10^{-5} s. The number of grids used in the simulation were 121×121 for the CFD code and 21×21 for the radiation code in r and z directions, respectively. The computations took approximately 36 hours of CPU time with 5 processors (each Pentium IV 2.66 GHz having 1 Gb of RAM).

Figs. 5 and 6 illustrate the steady-state temperature, axial component of velocity and selected species profiles for cases with and without radiation. As can be seen from Fig. 5(a), incorporation of radiation into the CFD code results in a decrease

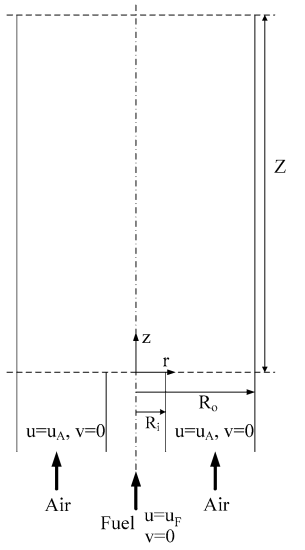

Geometrical Parameters:

$R_i = 0.635$ cm
$R_o = 2.54$ cm
$Z = 30$ cm

Operating conditions:

Pressure at the exit of the burner: $p = 1$ atm
Shield temperature: $T_w = 298$ K

Inlet streams:

i) Inner tube (Fuel side):
Inflow axial velocity: $u_F = 4.5$ cm/s
Inflow radial velocity: $v_F = 0.0$ cm/s
Temperature: $T_F = 298$ K
Composition: $Y_{CH_4} = 1.0$

ii) Outer tube (Oxidizer side):
Inflow axial velocity: $u_A = 9.88$ cm/s
Inflow radial velocity: $v_A = 0.0$ cm/s
Temperature: $T_A = 298$ K
Composition: $Y_{O_2} = 0.232$, $Y_{N_2} = 0.768$

Fig. 4. Details of the confined axisymmetric laminar diffusion flame burner.

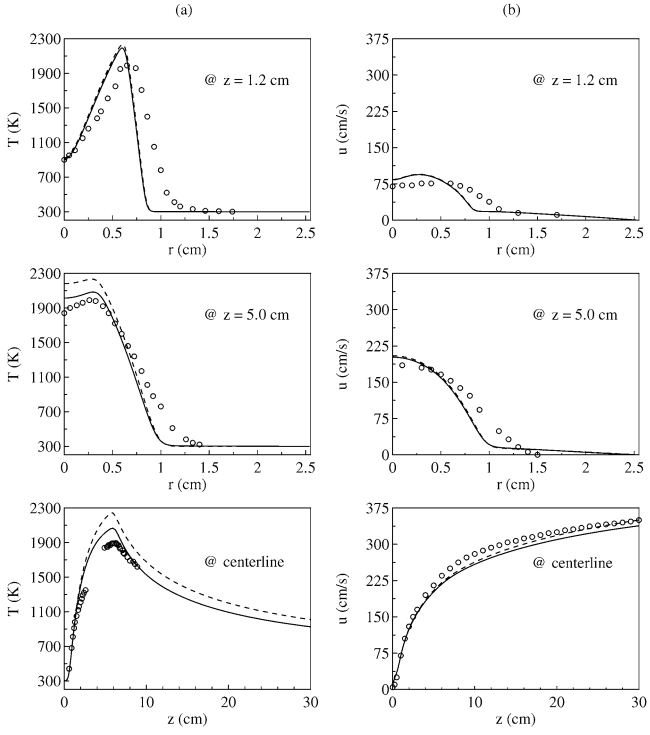

Fig. 5. Radial and axial profiles of temperature and axial component of velocity at two axial locations and along the centerline: (a) Temperature; (b) Velocity. Symbol: Experiment [12]; —— : With radiation; - - - : Without radiation [11].

in the predicted temperatures and significant improvement in agreement between the measured and predicted temperature fields compared to predictions without radiation [11]. The differences in the temperature fields predicted with and without radiation, correspond to minor discrepancies in the flow fields owing to the fact that variations in the density and viscosity of the reaction mixture are insignificant in the regions of the flow field where these temperature differences occur. Species profiles such as CO_2 and H_2O which are important in terms of radiative heat transfer (due to their absorbing emitting nature)

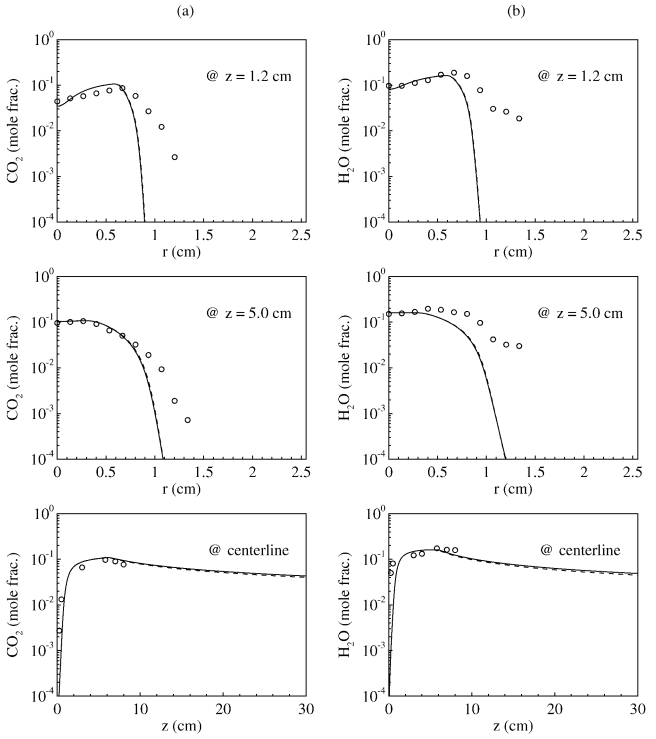

Fig. 6. Radial and axial profiles of CO_2 and H_2O mole fractions at two axial locations and along the centerline: (a) CO_2; (b) H_2O. Symbol: Experiment [12]; —— : With radiation; - - - : Without radiation [11].

are displayed in Fig. 6. It can be seen that species profiles predicted with and without radiative heat transfer are nearly the same. This may be attributed to the fact that species mole fractions are more sensitive to the reaction mechanism employed in the computations than to the temperature field.

In order to demonstrate the predictive ability of the algorithm developed in the present study for transient solutions, time development of velocity and temperature fields for the suddenly started diffusion flame are presented in Figs. 7 and 8. The burner is initially filled with air at room temperature and the flow is at rest. Fuel and air both at room temperature are allowed to enter the system and ignition takes place at the intersection region of fuel and air by providing a small hot region (which is at 1500 K) higher than the ignition threshold value for a time period of 50 m s. Combustion starts immediately and flame propagates to the burner exit.

Fig. 7 shows the time development of the axial velocity by color contours and streamlines. As can be seen from the figure, as soon as flow is started, the velocity increases in the inlet region along the centerline due to increase in temperature. The flow starts to separate downstream yielding two large recirculation cells that are established between the hot flame region and the cold wall. At steady-state these recirculation cells take their final forms remaining in the system. Air is entrained into the system at the system outlet to balance the momentum of the inlet fuel and air streams along with the frictional losses at the shield wall. The presence of these recirculation cells reduces the total area available for the flow of the combustion gases and hence the velocities are increased due to the combined effects of natural convection and a reduced flow area. High velocity

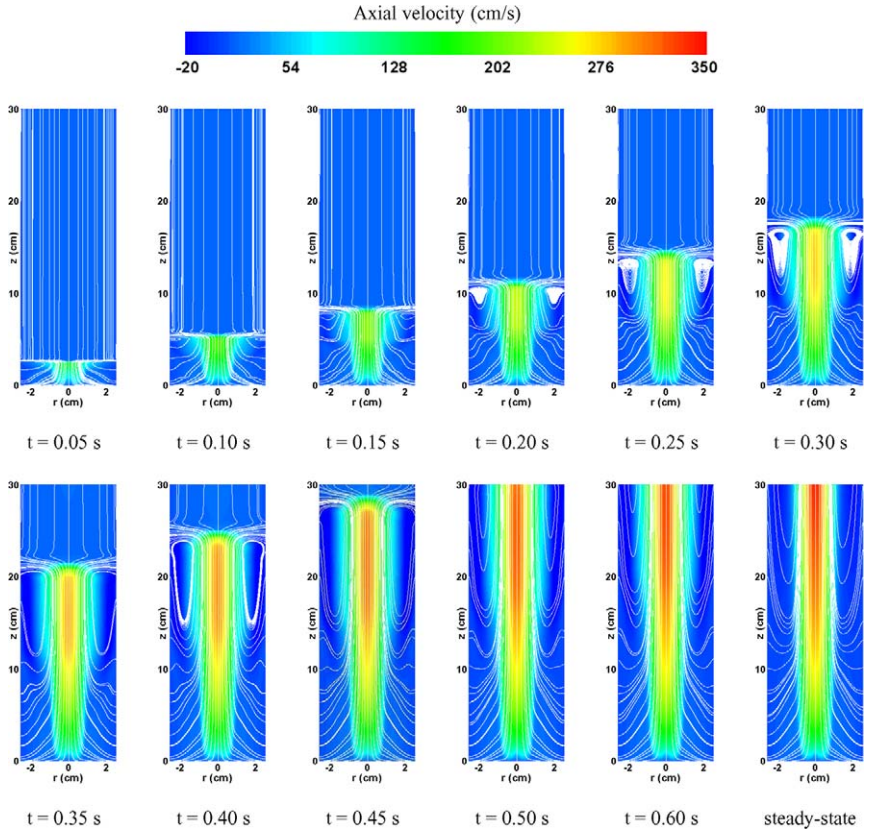

Fig. 7. Time development of streamline pattern and axial velocity field.

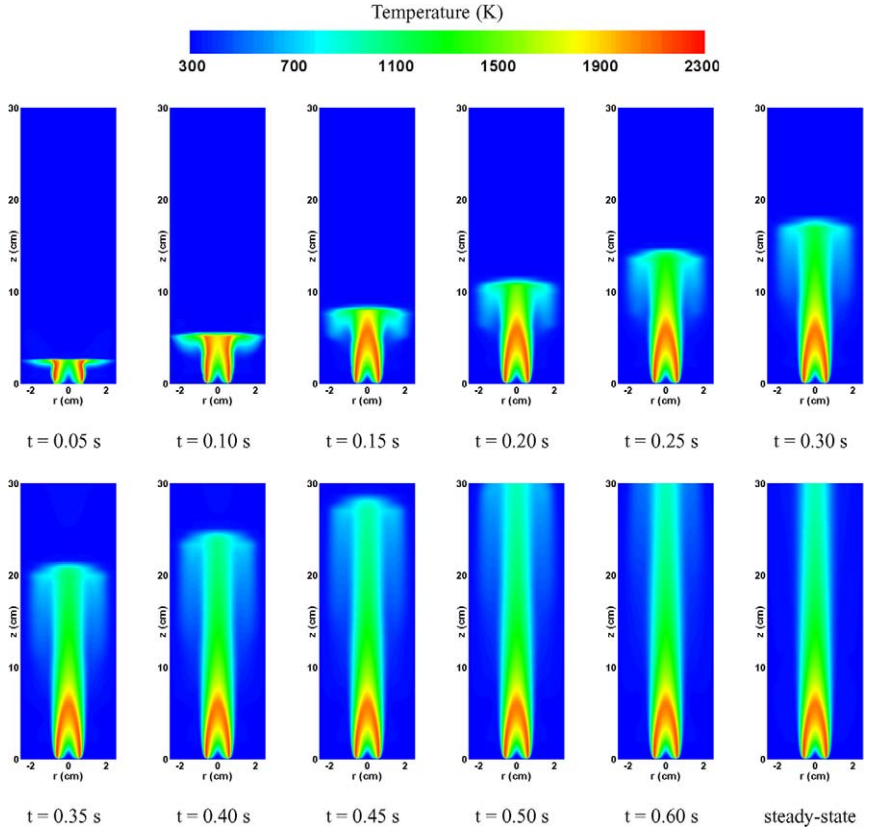

Fig. 8. Time development of temperature field.

gradients appear in the whole domain, axial velocity ranging in magnitude from $-20\ \mathrm{cm\,s^{-1}}$ to $350\ \mathrm{cm\,s^{-1}}$.

Time development of temperature field is shown in Fig. 8. As can be seen from the figure, as soon as flow is started, reaction starts to take place immediately and high temperature region extends from the boundary of the fuel and oxidizer jets to the symmetry axis. Thereafter, as the flow moves downstream, the temperature field broadens to the walls due to the recirculations. Recirculations cause the fuel and oxidizer to expand in the wall direction. As time progresses, fuel and oxidizer flow downstream resulting in the formation of the shape of a typical flame. After a distance from the inlet, fuel is depleted and therefore, temperature starts to decrease further downstream. In an attempt to compare the transient results of the present code with those of [11], it was seen that the temperatures predicted along the centerline region are lower than those reported in [11] as a consequence of radiative heat transfer from the center towards the wall.

5. Conclusion

An existing radiation code based on MOL solution of DOM was incorporated to a MOL based parallel DNS code for the simulation of methane–air confined diffusion flame problem. A global (one step) reaction mechanism was employed in the computations. The predictions of code were benchmarked against both experimental data and numerical results without radiation transport. Encouraging agreement between the predictions of the present code and measurements in terms of temperature field reveals the ability and the reliability of the coupling strategy utilized. The predictive ability of the algorithm for transient solutions was demonstrated and physically expected trends were observed. The code is a promising tool as it can be extended to the simulation of transient turbulent reacting and radiating flows by incorporation of detailed reaction mechanisms and improvement of the existing models.

Acknowledgements

(1) The numerical calculations reported in this paper were carried out at the ULAKBIM High Performance Computing Center at the Turkish Scientific and Technical Research Council (TUBITAK). The support is gratefully acknowledged.
(2) This study is partially supported by Middle East Technical University Scientific Research Projects Office.

References

[1] R. Hilbert, F. Tap, H. El-Rabii, D. Thevenin, Impact of detailed chemistry and transport models on turbulent combustion simulations, Prog. Energy Combust. Sci. 30 (2004) 61–117.
[2] C.R. Kaplan, S.W. Baek, E.S. Oran, J.L. Ellzey, Dynamics of a strongly radiating unsteady ethylene jet diffusion flame, Combust. Flame 96 (1994) 1–21.
[3] B. Bedat, F. Egolfopoulos, T. Poinsot, Direct numerical simulation of heat release and NO_x formation in turbulent non premixed flames, Combust. Flame 119 (1/2) (1999) 69–83.
[4] P.J. Coelho, O.J. Teerling, D. Roekaerts, Spectral radiative effects and turbulence/radiation interaction in a non-luminous turbulent jet diffusion flame, Combust. Flame 133 (2003) 75–91.
[5] F. Liu, H. Guo, G.J. Smallwood, Effects of radiation model on the modeling of a laminar coflow methane/air diffusion flame, Combust. Flame 138 (2004) 136–154.
[6] W.E. Schiesser, The Numerical Method of Lines: Integration of Partial Differential Equations, Academic Press, New York, 1991.
[7] O. Oymak, N. Selçuk, Method of lines solution of time-dependent two-dimensional Navier–Stokes equations, Int. J. Numer. Methods Fluids 23 (5) (1996) 455–466.
[8] N. Selçuk, O. Oymak, A novel code for the prediction of transient flow field in gas turbine combustor simulator, in: AVT Symposium on Gas Turbine Engine Combustion, Emission and Alternative Fuels, 12–16 October 1998, Lisbon, Portugal, NATO/RTO Meeting Proceedings 14 (11), pp. 1–10.
[9] T. Tarhan, N. Selçuk, Method of lines for transient flow fields, Int. J. Comput. Fluid Dynamics 15 (2001) 309–328.
[10] A. Bilge Uygur, T. Tarhan, N. Selçuk, Mol solution for transient turbulent flow in a heated pipe. I, J. Therm. Sci. 44 (2005) 726–734.
[11] T. Tarhan, Numerical simulation of laminar reacting flows, PhD thesis, Middle East Technical University, Turkey, 2004.
[12] R.E. Mitchell, A.F. Sarofim, L.A. Clomburg, Experimental and numerical investigation of confined laminar diffusion flames, Combust. Flame 37 (1980) 227–244.
[13] N. Selçuk, G. Kirbas, The method of lines solution discrete ordinates method for radiative heat transfer in enclosures, Numer. Heat Transfer Part B 37 (2000) 379–392.
[14] N. Selçuk, A. Batu, I. Ayranci, Performance of method of lines solution of discrete ordinated method in the freeboard of a bubbling fluidized bed combustor, J. Quant. Spectrosc. Radiat. Transfer 73 (2002) 503–516.
[15] N. Selçuk, I. Ayranci, The method of lines solution of discrete ordinates method for radiative heat transfer in enclosures containing scattering media, Numer. Heat Transfer Part B 43 (2003) 179–201.
[16] S. Harmandar, N. Selçuk, The method of line solution of discrete ordinated method for radiative heat transfer in cylindrical enclosures, J. Quant. Spectrosc. Radiat. Transfer 84 (4) (2004) 409–422.
[17] N. Selçuk, A. Bilge Uygur, I. Ayranci, T. Tarhan, Transient simulation of radiating flows, J. Quant. Spectrosc. Radiat. Transfer 93 (3) (2005) 151–161.
[18] E.E. Khalil, J.B. Spalding, J.H. Whitelaw, The calculation of local flow properties in two-dimensional furnaces, Int. J. Heat Mass Transfer 18 (1975) 775–791.
[19] R.J. Kee, G. Dixon-Lewis, J. Warnatz, M.E. Coltrin, J.A. Miller, A Fortran computer code package for the evaluation of gas-phase, multicomponent transport properties, Sandia Laboratories, SAND86-8646, 1986.
[20] R.J. Kee, F.M. Rupley, E. Meeks, J.A. Miller, Chemkin-III: A Fortran chemical kinetics package for the analysis of gas phase chemical and plasma kinetics, Sandia Laboratories, SAND96-8216, 1996.
[21] T. Tarhan, N. Selçuk, Numerical simulation of a confined methane/air laminar diffusion flame by method of lines, Turkish J. Engrg. Env. Sci. 27 (2003) 275–290, http://journals.tubitak.gov.tr/engineering/issues/muh-03-27-4/muh-27-4-8-0303-2.pdf.
[22] B. Leckner, Spectral and total emissivity of water vapor and carbon dioxide, Combust. Flame 19 (1978) 33–48.
[23] C. Ersahin, T. Tarhan, I.H. Tuncer, N. Selçuk, Parallelization of a transient method of lines Navier–Stokes code, Int. J. Comput. Fluid Dynamics 18 (1) (2004) 81–92.
[24] R. Weiner, B.A. Schmitt, H. Podhaisky, Rowmap—a row-code with Krylov techniques for large stiff odes, Technical Report, FB Mathematik und Informatik, Universitaet Halle, 1996.